International Journal of Engineering Trends and Technology
ISSN: 2231 – 5381 /doi:10.14445/22315381/IJETT-V68I12P225
Volume 68 Issue 12, 153-159, December 2020

Performance Analysis Of Wiener Filter With Different Window Functions In Detecting Broken Rotor Fault In 3 Phase Induction Motor

K. C. Deekshit Kompella[#1], Gopala Venu Madhav[*2]

[#]*Assistant Professor, Department of EEE, Sreenidhi Institute of Science & Technology, Hyderabad, India*
[*]*Professor, Department of EEE, Anurag Group of Institutions, Hyderabad, India*

[1]kkcd10@gmail.com, [2]venumadhaveee@cvsr.ac.in

Abstract - *Premature fault detection in induction motor has become popular due to its unavoidable relation with industries' financial and production aspects. Among the various faults endured, broken rotor bar (BRB) faults frequently occur in cage rotor type motors. These faults are difficult to identify in the current signature due to its spectral nearness. Therefore, many recent authors have concentrated on detecting these faults with no delay time and less complexity. Selection of proper filter with suitable window function is very crucial to achieve this and to elevate the series of sideband frequencies in the current spectrum. In this paper, the detection of BRB fault using Wiener filter (WF) with various window functions is presented. Performance of WF with these window functions is compared with classical WF using recorded signals of BRB fault from 1.5kW induction motor under different load conditions.*

Keywords — *Induction Motor, Rotor Faults, Current Signature Analysis, Wiener Filter, Window Functions.*

I. INTRODUCTION

For years, induction motors (IMs) are playing a crucial role in industries, especially in the production process and domestic purposes [1]-[2]. This is because of its unique advantages like reliability, low cost, stalwart structure, rugged design, and robustness [1], [2]. They are extensively used as prime movers in industries. The continued usage of an induction motor under the mechanical and electrical stresses and harsh environmental operating conditions leads to deterioration that can cause the development of various incipient faults. According to several surveys [3], the percentage occurrences of different faults in an induction motor are rotor-10, stator-38, bearing-40, and others-12. Though the percentage contribution of rotor faults is 10, it pays a considerable amount of time, money, etc., to get the motor to its original condition. The premature rotor faults may cause pulsations in torque, fluctuations in speed, vibrations, and leads to the development of new frequencies in the current spectrum and electromagnetic fields [4-5]. A defective, broken bar can increase the resistance, leads to overheating and physical damage of the rotor cage[4-6]. Though the damaged rotor may not be catastrophic, it requires to identify at the premature stage to avoid its development into more severe faults [4]. It is one of the most difficult faults to be detected. One of the common methods of detecting this fault is motor current signal analysis [7-12]. Though the fault detection using stray flux [13], acoustic signal [14], noise [15], and vibration signals [16] has given the best results, the MCSA become more popular in recent days due to its merits like simpleness, non-invasiveness, less manpower, and low cost, etc.

Broken rotor fault detection using MCSA becomes complicated due to its spectral nearness. Spectral nearness is the existence of fault frequencies as a series of sidebands for the fundamental component. This requires a perfect filter to elevate fault frequencies after removing the fundamental component in the current spectrum. Many researchers have concentrated on the elimination of these healthy components using adaptive Notch filter (NF) [17], Kalman filter (KF) [18], Extended Kalman Filter (EKF) [19-20], unscented Kalman filter (UKF)[21] and Taylor- Kalman Filter (TKF) [22]. Design of notch filter requires a proper bandwidth or Q-factor in eliminating the required frequency component. In this, the notch is provided at a fundamental frequency, which leads to the elimination of sidebands. Proper care is taken to save these sideband frequencies of stator current. As series of fault frequencies may also be developed at harmonics, notches should be provided at these harmonics and become complicated. Moreover, these notch frequencies change with respect to change in supply frequency due to power quality issues. This requires adaptiveness in filter design to choose the original fundamental frequency and its harmonics, which intern increases mathematical complexity. In view of this, Kalman Filter (KF) is proposed to detect the broken rotor bar [18]-[20] and have many limitations like linearization, mathematical complexity due to Jacobian Matrices [21], and requirement of large windows which intern maximize the time delay in BRB fault detection [22].

In view of this, Wiener Filter (WF) based fault detection is proposed in this paper and requires more modifications on conventional filter design [23]-[27]. Conventional Wiener filter in [23]-[24] is designed to detect all categories of bearing faults in induction motor and gives good results. To

improve the fault detection capability of WF, stationary wavelet transform is used in [25] and shows a better indication for fault. But the conventional WF removes the sidebands, which intern cancels BRB fault frequencies. To overcome this, proper window function is required to decrease the main lobe width and increase the height of the sidelobe to remain sideband frequencies. In [26], WF with the Kaiser window function is presented to identify bearing faults in the induction motor along with the fault indexing parameter. In continuation to this, detection of bearing, BRB, and combined faults using FSS and WF along with Kaiser window is presented in [27] and shows oscillating nature of the fault features under no-load condition. Therefore, in the present work, BRB defects of induction motor are estimated using MCSA via WF along with different window functions, and performance is compared. Moreover, the Matrix Pencil Method (MPM) [28]-[29] is employed for spectral analysis along with the feature parameter. The total process of fault detection is carried out at various load conditions to examine the reliability and accuracy of the proposed topology.

This paper is organized as fault detection topology along with the design of WF and application of MPM is presented in Section II, experimental procedure along with the exhibits of the experimental setup, faults used and table of fault frequencies for proposed BRB fault are presented in Section III. Experimental results are discussed in Section IV, and the conclusions are presented in Section V.

II. METHODOLOGY OF FAULT DETECTION

The detailed procedure of fault detection proposed in this paper is discussed in this section, and the flow diagram of the methodology is shown in Fig.1. As the first step of fault detection, the stator current of the induction motor under various health conditions is acquired using a data acquisition card with a suitable sampling rate. In the next step, noise along the acquired current is removed using wavelet de-noising [30]to make the

This work was supported in part by the JNTUH under Grant of TEQIp-III with section order JNTUH/TEQIP-III/CRS/2019/EEE04.

The system is robust. For this, the selection of threshold value, decomposition level, and mother wavelet is adopted from [31]. In the next step, the healthy components of the stator current spectrum are removed using a Wiener filter. The design of WF and its improvement using different window functions are discussed in the following subsection.

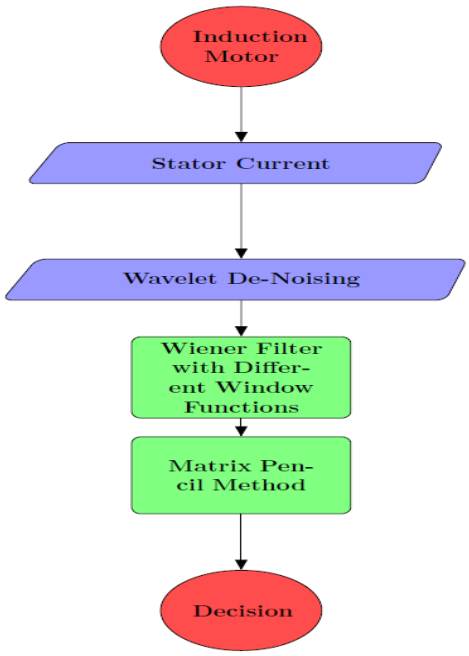

Fig.1. Fault detection methodology step ladder.

A. Design aspects of WF Coefficients

While designing the WFcoefficients, stator current healthy components like supply fundamental, its harmonics, and the noise remain after de-noising are modeled and trained to nullify the error between predicted frequencies by the filter and actual frequencies. This error is reduced using the minimum mean square method [23]-[27] and is given by

$$\delta = E\{|e(n)|^2\} = E\{\left|I(n) - \sum_{k=0}^{L-1} w(k) I_f(n - n_0 - k)\right|^2 \quad (1)$$

Where δ is an error, E {} is an expectation, I(n) is the modeled current in the time domain, m is the order of the filter, and I_f is the predicted current. This error is minimized by equating the derivative ofδ to zero.

$$\frac{\partial \delta}{\partial w(k)} = 0 \quad (2)$$

From equation (1) & (2)

$$\frac{\partial e(n)}{\partial w(k)} = -I_f(n - n_0 - k) \quad (3)$$

By simplifying equation (3) and from the principle of orthogonality, filter coefficients are given by

$$W = R_I^{-1} r_{dI} \quad (4)$$

Where R_I is the Toeplitz matrix of autocorrelation, and $_I$ am the cross-correlation function. These filter coefficients are modified using the Kaiser window function in [26], and the modified coefficients are

$$W_M = W .* K(n) \quad (5)$$

In this paper, instead of the Kaiser window, different windows, namely Blackman Harris [32], Hanning, Blackman, Bartlett, are used, and the performance of the filter with these windows are compared with Kaiser window and conventional coefficients. Mathematical expressions for these window functions are presented in the following.

$$K(n) = \frac{I_0\left[\beta\sqrt{\left(\frac{L-1}{2}\right)^2-\left(n-\frac{L-1}{2}\right)^2}\right]}{I_0\left(\beta\left(\frac{L-1}{2}\right)\right)} (6)$$

$$BH(n) = 0.358 - 0.488\cos\left(\frac{2\pi n}{L-1}\right) + 0.141\cos\left(\frac{4\pi n}{L-1}\right) - 0.011\cos\left(\frac{6\pi n}{L-1}\right) (7)$$

$$H(n) = 0.5 - 0.5\cos\left(\frac{2\pi n}{L-1}\right) \quad (8)$$

$$B(n) = 0.42 - 0.5\cos\left(\frac{2\pi n}{L-1}\right) + 0.08\cos\left(\frac{4\pi n}{L-1}\right) (9)$$

$$T(n) = 1 - \frac{2\left|n-\frac{L-1}{2}\right|}{L-1} (10)$$

Where L is the length of the filter, K(n) is Kaiser window, BH(n) is Blackman Harris window, H(n) is Hanning window, B(n) is Blackman window, and T(n) is Bartlett window functions. Each window function from equation (6) to (10) is substituted in (5) one by one, and corresponding filter coefficients are saved from removing the healthy components. After removing these components from the stator current, the residual components are used to reconstruct the signal. Further, this is used for spectral analysis using MPM to estimate the fault frequency components. The detailed procedure of spectral analysis using MPM is discussed in the following subsection.

Matrix Pencil method (MPM):

In the MPM, the frequency domain analysis of stator current is performed after WFC. The fault components, along with their magnitudes, are separated using pencil matrices. The mathematical expressions to develop the current spectrum are adopted from [27],[29], and mentioned here. The expression for motor current after removing acompobove mentioned components is

$$I_r(n) = I_\alpha(n) + \sum_{j=1}^{N} I_j(n)\sin\left(\omega_{fj}\, n/F_s\right) (11)$$

Where $I_\alpha(n)$ is the noise in the current, $I_j(n)$ is the magnitude of fault component, ω_{fj} is angular fault frequencies, and F_s is the sampling rate. Now the current in equation (11) is used for MPM, and the following matrix of magnitude and phase value of each fault component is developed.

$$\begin{bmatrix} I_{r1} \\ I_{r2} \\ \vdots \\ I_{r(M-L)} \end{bmatrix} = \begin{bmatrix} 1 & 1 & \dots & 1 \\ z_1 & z_2 & \dots & z_N \\ \vdots & \vdots & \vdots & \vdots \\ z_1^{M-1} & z_2^{M-1} & \dots & z_N^{M-1} \end{bmatrix} \begin{bmatrix} R_1 \\ R_2 \\ \vdots \\ R_N \end{bmatrix} (12)$$

Where N is the order of the pencil matrix, and L is the pencil value. After MPM, the residual components are used for the evaluation of feature value to estimate the severity of the BRB fault. MS value of residual current after MPM is taken as a feature parameter, and the fault indexing is evaluated by considering the ratio between RMS value of fault current to RMS value of healthy current. The complete experimental details are discussed in the following section.

III. EXPERIMENTAL TESTING

In the experimental verification of proposed fault detection, 2HP, 3.5A star connected, 415V, 50Hz, and 1430 rpm full load speed of 3 phase induction motor is chosen. The motor is with a cylindrical cage rotor and loaded with a spring balance. Motor current is sensed by LEM LA55P and acquired using NI MyRIO make by National Instruments in the LabVIEW environment. The total arrangement of testing equipment is presented in Fig.2. A sampling rate of 10kHz with 10000 samples of current is collected at every time. As a part of the experimental procedure, the stator current under normal operating conditions is measured, and the proposed fault detection procedure is applied in the MATLAB. The corresponding feature parameter is computed for reference. In the next part, the cage rotor is drilled with a hole of 5mm on the end ring, and corresponding features are measured. Further, the cage rotor is drilled with 2 holes of 5mm on the cylindrical part, and the total procedure is repeated. The complete picture of rotor faults is exhibited in Fig.3. The complete experiments are conducted at No-load, Full load, and two more loads between them. The currents at load 1-4 are 2.1A, 2.5A, 2.75A, and 3.5A, respectively, and the corresponding speeds are 1498rpm, 1485rpm, 1475rpm, and 1450rpm. The series of fault frequencies in stator current spectrum by BRB fault is given by [22]

$$f_{BRB} = f_s(1 \pm 2ks) (13)$$

Where f_{BRB} is the characteristic fault frequency developed by BRB fault, f_s is supplied fundamental, s is the per-unit slip, and k is the harmonic order. For the above-mentioned operation, the fault frequencies are calculated and presented in Table.1.The complete analysis of experimental results at different load conditions is discussed in the following section.

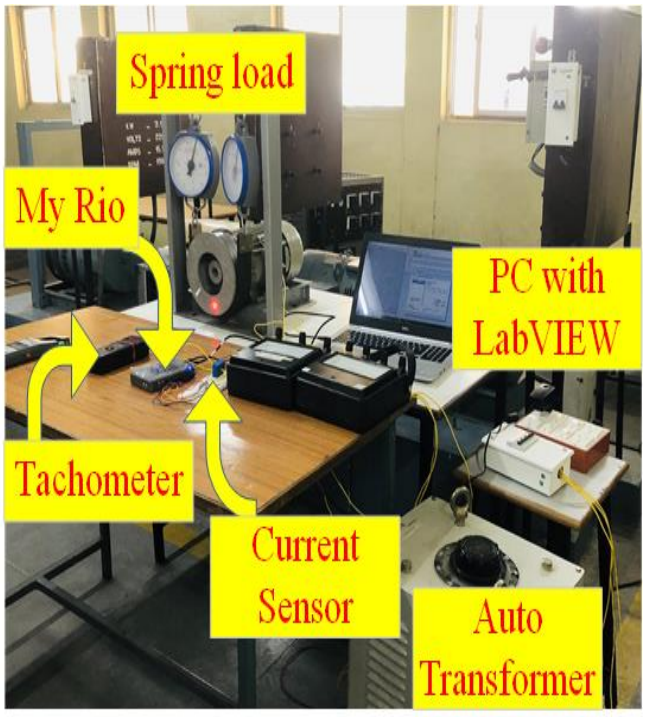

Fig.2. Exhibition of experimental equipment

Fig.3. Fault exhibits used in experimental verification

Table. I
Characteristic fault frequencies due to BRB fault in Hz.

Load	k=1		k=2		k=3		k=4	
	S-1	S-2	S-1	S-2	S-1	S-2	S-1	S-2
Load-1 (No-Load)	50.06	49.93	50.13	49.87	50.19	49.80	50.26	49.74
Load-2	50.5	49.5	51	49	51.5	48.5	52	48
Load-3	50.8	49.2	51.66	48.34	52.49	47.51	53.32	46.68
Load-4 (Full Load)	51.65	48.33	53.3	46.7	54.95	45.05	56.6	43.4

IV. EXPERIMENTAL RESULTS & DISCUSSION

The stator current normal operating condition of the machine is acquired at different load conditions and stored offline. In the same way, stator currents at proposed faulty conditions are also measured at different loads are stored. The stator current in time domain analysis under no-load condition is shown in Fig.4.It is critical to identify the defect due to its identical nature. Therefore, frequency domain analysis of motor current is done at all load conditions and presented in Fig.5 to 6, and it is observed that domination of healthy components suppressing the fault component, especially at no load. As presented in Table.1, the fault frequencies are away from the fundamental component as the speed decreases with increment in load.

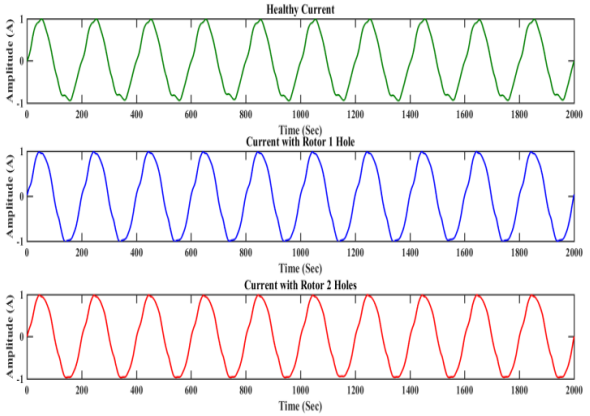

Fig.4. Stator current with the normal and abnormal condition at no-load

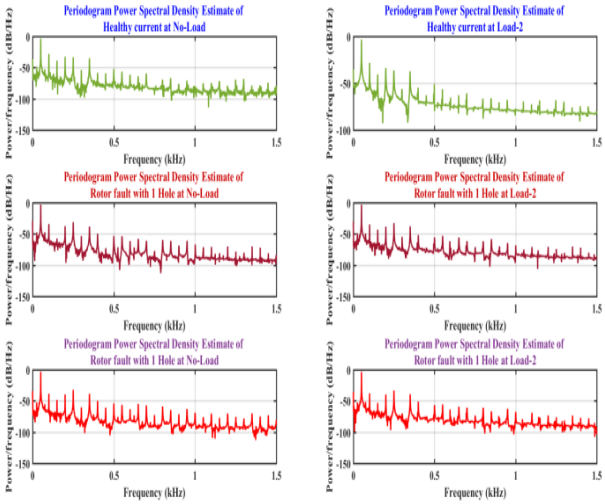

Fig.5. Stator current spectrum under no-load & Load2.

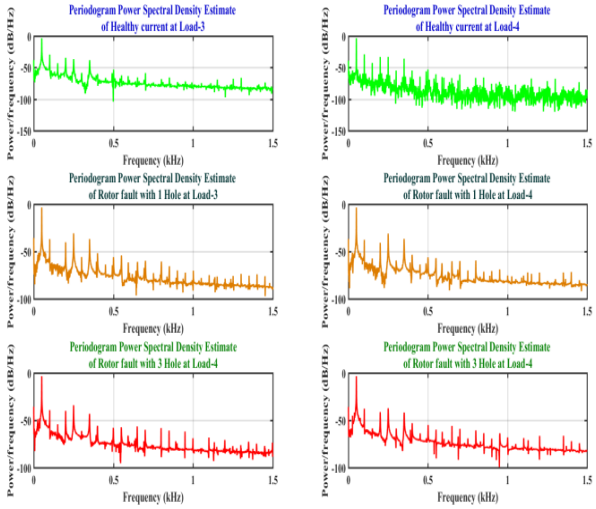

Fig.6. Stator current spectrum under load-3 & full load.

From the power spectrum of stator currents at different load conditions, it is observed that the spectrum consists fundamentally, and it's all harmonics like even and odd due to problems in design aspects. Along with this, the fault frequencies due to BRB will exist in a few cases with less magnitude. This is due to the domination of regular components. Therefore, wiener filter cancellation is implemented as mentioned in the above section. The power spectrum of motor current after wiener filter cancellation is mentioned in Fig. 7 to 9. Each load case is separately plotted and observed that all the dominant frequencies are successfully eliminated, and fault frequencies are elevated. Various windows proposed in section-2 are used in filter design, which is presented in Fig.7. At no-load, conventional filtering with Blackman and Kaiser window have shown better performance compared to Blackman Harris, Hanning, and Bartlett window as the healthy components remain even after wiener filter cancellation using these windows. But completely removed using rectangular, Blackman, and Kaiser windows. The same will be shown for both faulty conditions of rotor 1 and 3 holes, as shown in Fig.8 and 9. Both the faulty cases will show the same results that the healthy components are perfectly eliminated using windows like healthy cases. Moreover, few faulty frequencies are elevated using few windows, but severity estimation is difficult due to per unit estimation of the current signal. To estimate the severity of the fault, the RMS value is computed after MPM. The bar diagram of RMS values for all cases of the motor at the proposed loads are presented in Fig.10 and 11.

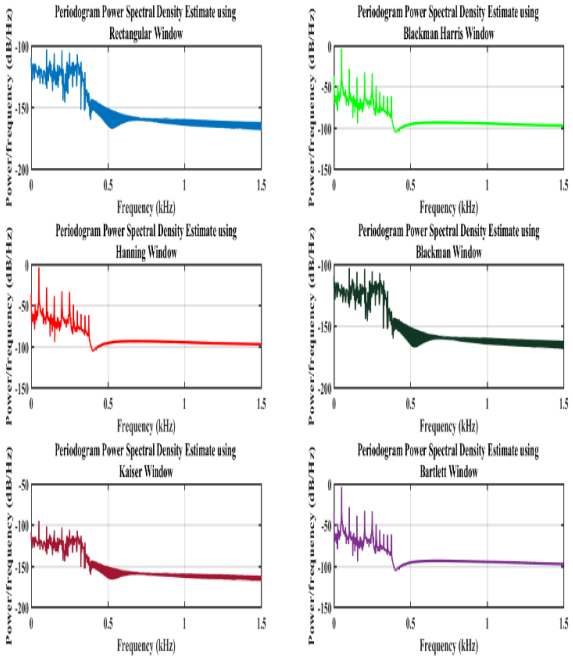

Fig.7. Stator current spectrum under no-load after the cancellation of healthy components at normal condition.

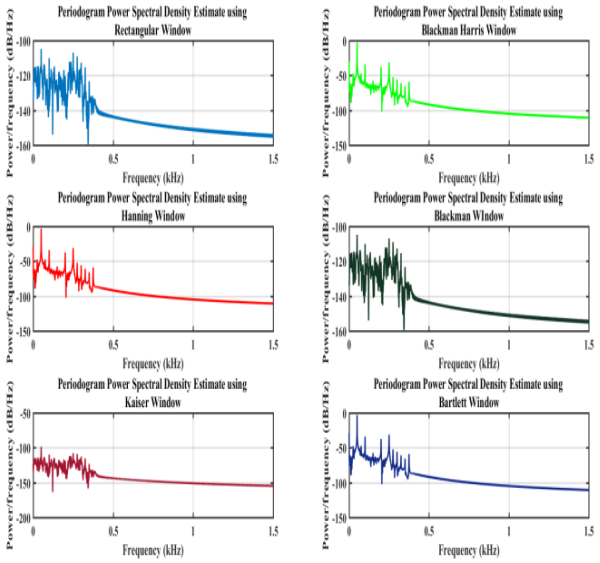

Fig.8. The power spectrum of stator current under no-load after the cancellation of healthy components at rotor fault condition with 1 hole.

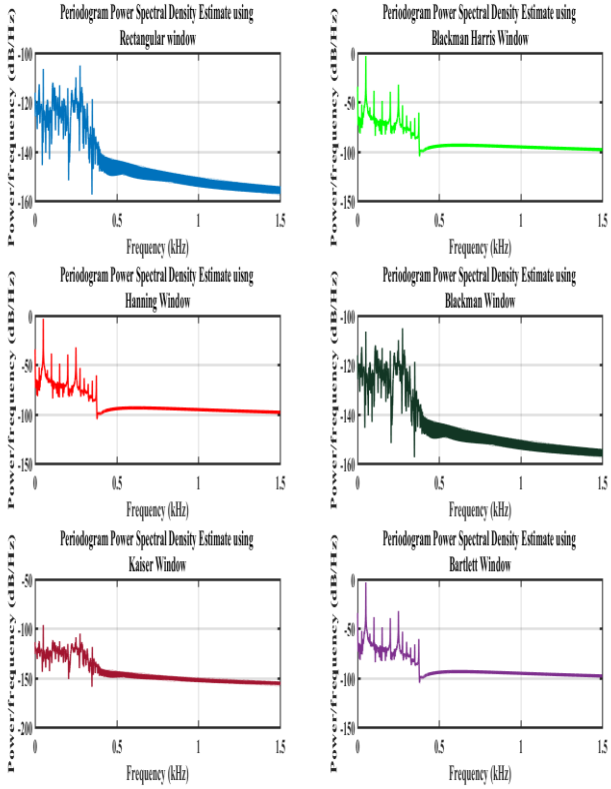

Fig.9. Stator current spectrum under no-load after the cancellation of healthy components at rotor fault condition with 1 hole.

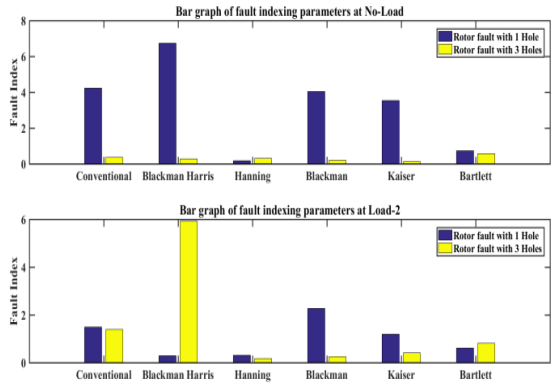

Fig.10. Bar graph of fault indexing parameter at no load and load-2.

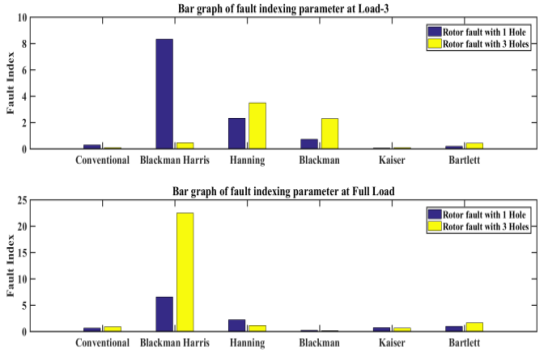

Fig.11. Bar graph of fault indexing parameter at load-3 and full load.

From the bar graphs of the fault indexing parameter, it is observed that the rotor faults are estimated using the Blackman Harris window for all the load conditions. In no-load condition, conventional filter along with Blackman harris, Blackman, and Kaiser window has shown good indication for fault at end ring. Whereas the motor is operating from no load to full load, only Blackman harris will maintain the indication, and hence it is suitable for all conditions of the load. The mesh diagrams of each fault are presented in Fig.12 and 13.

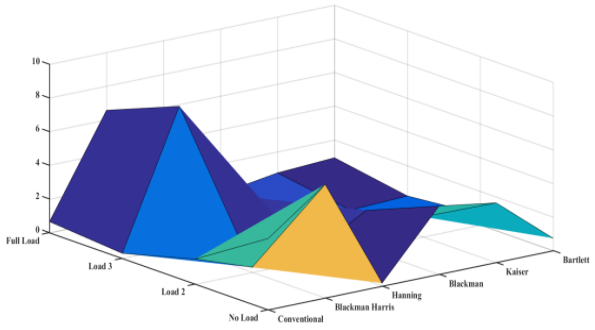

Fig.12. Mesh diagram of rotor fault with 1 hole using different windows

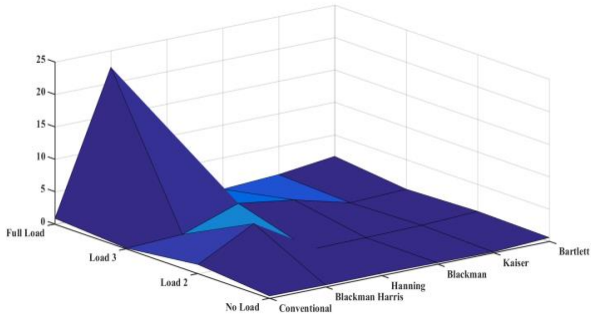

Fig.13. Mesh diagram of rotor fault with 3 holes using different windows

VI. CONCLUSIONS

This work presents a broken rotor fault estimation using current signature analysis with wiener filter cancellation. The filter performance is analyzed using different window functions, and residual currents are used for spectral analysis using the matrix pencil method. Finally, the feature parameter RMS value is taken to predict the seriousness of the fault. Blackman harris window has given sufficient indication for rotor fault at all the load conditions of the motor. Whereas remaining filters have shown good indication for fault at few load conditions and at some other, have shown poor performance. This may give an unreliable diagnosis of the machine and requires improper maintenance. Therefore, Wiener filter cancellation along with Blackman harris window is used for reliable fault detection in 3 phase induction motors. The experimental results have confirmed the perfectness of the proposed topology. Further, WFcoefficients may be computed by better minimization methods and tested for all categories of faults experienced by the motor.

REFERENCES

[1] Y. Li, X. Wang, Z. Liu, X. Liang, and S. Si, The Entropy Algorithm and Its Variants in the Fault Diagnosis of Rotating Machinery: A Review, in IEEE Access, 6(6) (2018) 6723-66741, doi: 10.1109/ACCESS.2018.2873782.

[2] Liu, R., Yang, B., Zio, E., and Chen, X.,. Artificial intelligence for fault diagnosis of rotating machinery: A review. Mechanical Systems and Signal Processing, 108 (2018) 33-47.

[3] Singh, G., and Naikan, V.N.A.. Detection of half-broken rotor bar fault in VFD has driven induction motor drive using motor square current MUSIC analysis. Mechanical Systems and Signal Processing, 110 (2018) 333-348.

[4] Mirzaeva, G., and Saad, K.I.. Advanced diagnosis of rotor faults and eccentricity in induction motors based on internal flux measurement. IEEE Transactions on Industry Applications, 54(3) (2018) 2981-2991.

[5] Glowacz, Adam. Acoustic based fault diagnosis of three-phase induction motor. Applied Acoustics 137 (2018) 82-89.

[6] Quiroz, J.C., Mariun, N., Mehrjou, M.R., Izadi, M., Misron, N. and Radzi, M.A.M., 2018. Fault detection of broken rotor bar in LS-PMSM using random forests. Measurement, 116, pp.273-280.

[7] Jafari, H., and Poshtan, J.. Fault detection and isolation based on fuzzy-integral fusion approach. IET Science, Measurement & Technology, 13(2) (2018) 296-302.

[8] Ameid, T., Menacer, A., Talhaoui, H., and Azzoug, Y.. Discrete wavelet transform and energy eigenvalue for rotor bars fault detection in variable speed field-oriented control of induction motor drive. ISA transactions, 79 (2018) 217-231.

[9] Martin-Diaz, I., Morinigo-Sotelo, D., Duque-Perez, O., Osornio-Rios, R.A. and Romero-Troncoso, R.J.. Hybrid algorithmic approach oriented to incipient rotor fault diagnosis on induction motors. ISA transactions, 80 (2018)427-438.

[10] Morinigo-Sotelo, D., Romero-Troncoso, R.D.J., Panagiotou, P.A., Antonino-Daviu, J.A. and Gyftakis, K.N.. Reliable detection of rotor bars breakage in induction motors via MUSIC and ZSC. IEEE Transactions on Industry Applications, 54(2), (2017)1224-1234.

[11] Ramirez-Nunez, J.A., Antonino-Daviu, J.A., Climente-Alarcón, V., Quijano-Lopez, A., Razik, H., Osornio-Rios, R.A. and Romero-Troncoso, R.D.J., 2018. Evaluation of the detectability of electromechanical faults in induction motors via transient analysis of the stray flux. IEEE Transactions on Industry Applications, 54(5), pp.4324-4332.

[12] Morales-Perez, C., Rangel-Magdaleno, J., Peregrina-Barreto, H., Amezquita-Sanchez, J.P., and Valtierra-Rodriguez, M., 2018. Incipient broken rotor bar detection in induction motors using vibration signals and the orthogonal matching pursuit algorithm. IEEE Transactions on Instrumentation and Measurement, 67(9), pp.2058-2068.

[13] Park, Y., Yang, C., Kim, J., Kim, H., Lee, S.B., Gyftakis, K.N., Panagiotou, P.A., Kia, S.H. and Capolino, G.A., 2018. Stray flux monitoring for reliable detection of rotor faults under the influence of rotor axial air ducts. IEEE Transactions on Industrial Electronics, 66(10), pp.7561-7570.

[14] Glowacz, A., 2019. Fault diagnosis of single-phase induction motor based on acoustic signals. Mechanical Systems and Signal Processing, 117, pp.65-80.

[15] J. Zarei, E. Kowsari, and R. Razavi-Far, Induction Motors Fault Detection Using Square-Root Transformed Cubature Quadrature Kalman Filter, in IEEE Transactions on Energy Conversion, 34(2) (2019) 870-877, doi: 10.1109/TEC.2018.2877781.

[16] M. Rayyam, M. Zazi and Y. Hajji, Detection of broken bars in induction motor using the Extended Kalman Filter (EKF), Third World Conference on Complex Systems (WCCS), Marrakech, 2015, pp. 1-5, doi: 10.1109/ICoCS.2015.7483235.

[17] M. Rayyam, M. Zazi, Y. Hajji, and I. Chtouki, Stator and rotor faults detection in Induction Motor (IM) using the Extended Kaman Filter (EKF), 2016 International Conference on Electrical and Information Technologies (ICEIT), Tangiers, (2016), 148-152, doi: 10.1109/EITech.2016.7519579.

[18] E. Ghahremani and I. Kamwa, Online state estimation of a synchronous generator using unscented kalman filter from phasor measurements units, IEEE Transactions on Energy Conversion, 26(4) (2011) 1099–1108.

[19] L. A. Trujillo-Guajardo, J. Rodriguez-Maldonado, M. A. Moonem, and M. A. Platas-Garza, A Multiresolution Taylor–Kalman Approach for Broken Rotor Bar Detection in Cage Induction Motors, in IEEE Transactions on Instrumentation and Measurement, 67(6), (2018) 1317-1328, doi: 10.1109/TIM.2018.2795895.

[20] W. Zhou, B. Lu, T. G. Habetler and R. G. Harley, Incipient Bearing Fault Detection via Motor Stator Current Noise Cancellation Using Wiener Filter, in IEEE Transactions on Industry Applications, 45(4) (2009) 1309-1317, doi: 10.1109/TIA.2009.2023566.

[21] K. C. Deekshit Kompella, M. V. G. Rao, R. S. Rao, and R. N. Sreenivasu, Estimation of nascent stage bearing faults of induction motor by stator current signature using adaptive signal processing, 2013 Annual IEEE India Conference (INDICON), Mumbai, (2013) 1-5, doi: 10.1109/INDCON.2013.6725956.

[22] K. C. D. Kompella, M. V. G. Rao and R. S. Rao, "SWT based bearing fault detection using frequency spectral subtraction of stator current with and without an adaptive filter," TENCON 2017 - 2017 IEEE Region 10 Conference, Penang, 2017, pp. 2472-2477, doi: 10.1109/TENCON.2017.8228277.

[23] Kompella, KC Deekshit, Srinivasa Rao Rayapudi, and Naga SreenivasuRongala(In Press). Investigation of Bearing faults in three-phase Induction motor using Wavelet De-Noising with improved Wiener Filtering. International Journal of Power and Energy Conversion (Inderscience) (2020) (Accepted).

[24] Kompella, KC Deekshit, Naga SreenivasuRongala, Srinivasa Rao Rayapudi, and Venu Gopala Rao Mannam. Robustification of Fault Detection Algorithm in a 3 Phase Induction Motor using MCSA for various Single and Multiple Faults. IET Electrical Power Application (2020) (Accepted).

[25] Z. Liu and J. Huang, Adaptive matrix pencil method for mixed rotor faults diagnosis, 2016 XXII International Conference on Electrical Machines (ICEM), Lausanne, 2016, pp. 2158-2164, doi: 10.1109/ICELMACH.2016.7732821.

[26] K. C. Deekshit Kompella and G. V. Madhav, An Improved Matrix Pencil Method based Bearing Fault detection in Three Phase Induction Motor, 2020 IEEE International Conference on Computing, Power and Communication Technologies (GUCON), Greater Noida, India, (2020), 51-56, doi: 10.1109/GUCON48875.2020.9231196.

[27] Z. Li, T. Wang, Y. Wang, Y. Amirat, M. Benbouzid, and D. Diallo, A Wavelet Threshold Denoising-Based Imbalance Fault Detection Method for Marine Current Turbines, in IEEE Access, 8, (2020) 29815-29825, doi: 10.1109/ACCESS.2020.2972935.

[28] S. H. Mortazavi and S. M. Shahrtash, Comparing the de-noising performance of DWT, WPT, SWT, and DT-CWT for Partial Discharge signals, 43rd International Universities Power Engineering Conference, Padova, (2008) 1-6, doi: 10.1109/UPEC.2008.4651625.

[29] X. WANG, K. LEI, X. Yang, M. Li, and X. Wang, Harmonic Analysis Based on Blackman-Harris Self-Multiplication Window, 2020 5th Asia Conference on Power and Electrical Engineering (ACPEE), Chengdu, China, (2020), 2165-2169, doi: 10.1109/ACPEE48638.2020.9136197.